Renewable and Sustainable Energy Reviews 20 (2013) 353–363

Contents lists available at SciVerse ScienceDirect

Renewable and Sustainable Energy Reviews

journal homepage: www.elsevier.com/locate/rser

CFD applications for latent heat thermal energy storage: a review

Abduljalil A. Al-abidi *, Sohif Bin Mat, K. Sopian, M.Y. Sulaiman, Abdulrahman Th. Mohammed

Solar Energy Research Institute, University Kebangsaan Malaysia, Bangi 43600, Selangor, Malaysia

A R T I C L E   I N F O

Article history:
Received 1 July 2012
Accepted 19 November 2012
Available online 9 January 2013

Keywords:
Phase change material
Thermal energy storage
CFD
Fluent

A B S T R A C T

Thermal energy storage is needed to improve the efficiency of solar thermal energy applications (STEA) and to eliminate the mismatch between energy supply and energy demand. Among the thermal energy storages, the latent heat thermal energy storage (LHTES) has gained much attention because of its high-energy densities per unit mass/volume at nearly constant temperatures. This review presents previous studies on the numerical modeling of phase change materials (PCMs) through a commercial computational fluid dynamic (CFD) software and self-developed programming to study the heat transfer phenomena in PCMs. The CFD (Fluent) software is successively used to simulate the application of PCMs in different engineering applications, including electronic cooling technology, building thermal storage, and heating, ventilation, air conditioning (HVAC). Using CFD software to design LHTES is believed to be an effective way to save money and time and to deliver optimization tools for maximum efficiency of STEAs.

Contents

1. Introduction

Researchers intensively studied the thermal energy storage of PCMs for the last three decades because of the latter's high thermal energy densities per unit volume/mass and their applicability to different engineering fields using wide temperature ranges. PCM thermal storage plays a key role in improving energy efficiency. It limits the discrepancy between the energy supply and the energy demand of solar thermal energy applications (STEAs), particularly when the STEA operation strategy depends solely on solar energy as a main source. PCM thermal storage indicates high performance and dependability with the advantages of high storage capacity and nearly constant thermal energy [1]. Most STEAs need constant or near-constant temperature for high-efficiency strategies. Using latent heat thermal energy storage (LHTES) as thermal energy storage can provide the required

* Corresponding author. Tel.: +60 14 7169 139; fax: +60 38 9214 593.
E-mail address: abo_anas4@yahoo.com (A.A. Al-abidi).

1364-0321/$ - see front matter © 2012 Elsevier Ltd. All rights reserved.
http://dx.doi.org/10.1016/j.rser.2012.11.079

Nomenclature

C	Mushy zone constant (kg/m^3 s)
Cp	Specific heat of PCM, (J/kg)
g	gravity acceleration, (m/s^2)
h	sensible enthalpy(J/kg)
H	enthalpy (J/kg)
L	latent heat fusion (J/kg)
k	thermal conductivity (W/m K)
T	Temperature (°C or K)
u	velocity (m/s)

Greek letters

P	fluid density (kg/m^3)
γ	liquid fraction
β	volumetric expansion coefficient (1/K)
μ	Dynamic viscosity (kg/m s)
α	Phase volume fraction

Subscripts

ref	Reference
s	Solidus of the phase change materials
l	Liquidus of the phase change material

constant temperature that matches the melting temperature of the PCMs. PCMs are used in different engineering fields, such as in the following: the thermal storage of building structures [3–7]; building equipment, including domestic hot water; heating and cooling systems [8,9]; electronic products [10–12]; drying technology [13], waste heat recovery [14]; refrigeration and cold storage [15–18]; solar air collectors[19]; and solar cookers [20]. Using a CFD software to design a LHTES is expected to be an effective way to save money and time and to deliver optimization tools for maximum efficiency of STEAs.

2. Numerical solution of PCMs

The mathematical formulation of a phase transient known as a phase change or moving boundary is governed by a partial deferential equation that can be solved either analytically or numerically. The analytical solution of PCMs is problematic because of the nonlinear phase front interfaces, complex geometries, and nonstandard boundary condition; the few analytical studies available are on 1D cases with regular geometries and a standard boundary condition. Özisik [21] reported that the numerical method for solving PCMs can be categorized as fixed-grid, variable grid, front-fixing, adaptive grid generation, and enthalpy methods.

Predicting the behavior of phase change systems is difficult because of its inherent non-linear nature at moving interfaces, for which the displacement rate is controlled by latent heat lost or absorbed at the boundary [22]. The heat transfer phenomena in solid–liquid PCMs can be analyzed using two main methods: the temperature-based and enthalpy-based methods. In the first method, temperature is considered a sole dependent variable. The energy conservation equations for the solid and liquid are written separately; thus, the solid–liquid interface position can be tracked explicitly to achieve an accurate solution for the problems.

$$\frac{\partial T_s}{\partial n}k_s = \frac{\partial T_l}{\partial n}k_l + \rho L k v_n, \quad (1)$$

where T_s denotes the temperature in the solid phase, T_l denotes the temperature in the liquid phase, k_s is the thermal conductivity of the solid phase, k_l is the thermal conductivity of the liquid phase, n is the unit normal vector to the interface, and v_n is the normal component of the velocity of the interface. L is the latent heat of freezing, as shown in Fig. 1.

In the second method, the solid–liquid interface position need not be tracked. Researchers often use the enthalpy formulation because of the following advantages: (1) the governing equations are similar to the single-phase Eq.; (2) no explicit conditions need to be satisfied at the solid–liquid interface; (3) the enthalpy formulation involves the solution within a mushy zone, involving both solid and liquid materials, between the two standard phases; and (4) the phase change problem can be solved more easily [23].

$$\frac{\partial(\rho H)}{\partial t} + \nabla\cdot(\rho \overline{v} H) = \nabla\cdot(k\Delta T) + S \quad (2)$$

Where T denotes the temperature, k is the thermal conductivity, ρ is the density of the PCM, $\overline{v}$ is the fluid velocity, and H is the enthalpy, S is the source term.

Dutil et al. [22] presented an intensive mathematical and numerical review of the PCM application based on the first and second laws of thermodynamics. Using 252 references, they determined the mathematical and numerical methods applied to solve heat transfer problems involving PCMs for thermal energy storage, the mathematical fundamentals of PCMs, and the different application geometries and applications. Verma et al. [24] also introduced other PCM mathematical reviews.

Recently, researchers used the Fluent software by ANSYS to simulate melting and solidification in engineering problems. Other software that can be used to simulate the PCM process include COMSOL Multiphysics and Star-CMM+. However, Fluent is preferred by most researchers for melting and solidifying PCMs. Conversely, some researchers self-developed a program using computational language (C++, Fortran, Matlab) to study the heat transfer phenomena in PCMs. Table 1 summarizes some of the self-developed programs for different PCM geometries.

2.1. Fluent program

The Fluent software by ANSYS is a computational fluid dynamic (CFD) program used successfully to simulate different engineering problems. This software has a specific model that can simulate a range of different melting and solidification problems in engineering, including casting, melting, crystal growth, and

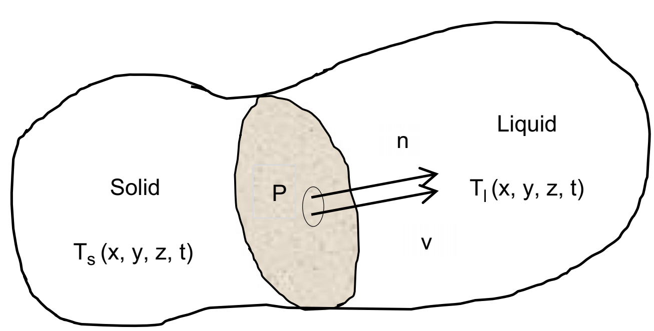


Fig. 1. Solid–liquid interface for a multidimensional situation [21].

Table 1
Self-developed numerical model for different PCM geometries.

Ref	PCM	Geometry	Dimension	Discretization methods	Numerical solution methods	Validation
[66]	Gallium	Rectangular	2D (X, Y)	FDM	Enthalpy method-based control volume approach; the power law used for discretization and semi-implicit method for pressure-linked equations (SIMPLE) was adopted for the pressure–velocity couple and for the tridiagonal matrix algorithm (TDMA) solver to solve the algebraic equations	Experimental
[67]	n-Octadecane	Rectangular	1D (X) 2D (X, Y)	FDM	An enthalpy formation-based control volume approach, the fully implicit method, and TDMA were used to solve the algebraic equations	[68,69]
[70]	Paraffin wax RII-56	PCM bags In duct	3D (X, Y, Z)	FDM	The interpolating cubic spline function method was used to determine the specific heat in each time step of the temperature calculations; the control volume approach and the backward Euler scheme were chosen for the temperature discretization in time	[71]
[72]	Paraffin RT30	Cylindrical	2D (R, X)	FVM	The power law used for discretization and SIMPLE were adopted for pressure–velocity coupling	Experimental
[73]	n-Octadecane	Cylindrical	2D (R, X)	FDM	Enthalpy methods and the TDMA solver were used to solve the equations	Experimental
[74]	4 PCM	Cylindrical	2D (R, X)	FDM	Fixed control volume and enthalpy methods	–
[75]	RT60	Cylindrical	2D (R, Θ)	FDM	A control volume-based implicit form was used. All equations were solved simultaneously using the Gauss–Seidel iterative method	Experimental
[76]	Paraffin 130/135 Type 1	Cylindrical	2D (R, Θ)	FDM	The enthalpy formulation approach, the control volume method, and the alternating direction scheme were used to discretize the basic equations	Experimental
[77]	Paraffin wax	Cylindrical	2D (R, Θ)	FDM	The control volume approach, the power law used for discretization, and the SIMPLE algorithm were adopted for pressure–velocity coupling	[78,79]
[80]	n-Hexacosane	Cylindrical	1D (R)	–	A temperature and thermal resistance iteration method was developed to analyze PCM solidification to obtain the solutions	Experimental
[81]	4PCM	Cylindrical	2D (R, X)	FDM	Enthalpy methods were used; the equations were solved simultaneously using the Gauss–Seidel iterative method	
[82]	2PCM	Cylindrical	2D (R, X)	FDM	The enthalpy method and the TDMA were used to solve the resulting algebraic equations solved using an iteration procedure	[73]
[83]	5 PCM	Cylindrical	2D (R, X)	FEM	Standard Galerkin finite element method was used	–
[84]	3 PCM	Cylindrical	2D (R, X)	FDM	Using the enthalpy method, the equations were solved by adopting the alternating direction implicit (ADI) method and the TDMA	[85]
[86]	Water	Spherical	1D (R)	FDM	An implicit FDM approach and a moving-grid scheme were used. The problem domain was divided into two regions, solid and liquid, both of which were separated by the interface. All algebraic equations were solved simultaneously	Experimental
[87]	Water, water Glycol mixtures	Spherical	1D (R)	FDM	The heat delivered by the capsule could also be calculated by the thermal resistance circuit. The resulting equation and associated boundary conditions were treated using a moving grid method	Experimental

FDM; Finite difference method, FEM; Finite elements method, FVM; Finite volume method.

solidification. The program can be used to solve the phase change that occurs at a single temperature (pure metals) or over a range of temperatures (mixture, alloy, and so on). The applications and limitations of Fluent can be found in Ref. [25].

To begin the Fluent software simulation, the physical engineering problem is drawn and meshed in a specific geometric modeling using mesh generation tools that include the Fluent software (Gambit, workbench). The mesh generation tools can be imported from other programs like Auto CAD. After the physical configuration is drawn and meshed, the boundary layers and zone types are defined, and the mesh is exported to the Fluent software.

Different grid sizes and time steps should be applied to the numerical model to ensure that the numerical results are independent of the parameters. Small grid sizes and time steps are preferred for a short simulation time in the computer.

2.2. Mathematical formulation for Fluent

The mathematical equations used to solve the solidification and melting models in Fluent depend on the enthalpy–porosity technique [26–28] and on the finite volume methods. In the former, the melt interface is not tracked explicitly. A quantity called liquid fraction, which indicates the fraction of the cell volume in liquid form, is associated with each cell in the domain. The liquid fraction is computed at each iteration based on enthalpy balance. The mushy zone is a region wherein the liquid fraction lies between 0 and 1. The mushy zone is modeled as a "pseudo" porous medium in which the porosity decreases from 1 to 0 as the material solidifies. When the material has fully solidified in a cell, the porosity becomes zero, resulting in the drop of velocities to zero. In this section, an overview of the solidification/melting theory is given. For details on the enthalpy–porosity method, refer to Voller and Prakash [26].

The energy equation is expressed as

$$\partial_t(\rho H)+\nabla(\rho\overline{v}H)=\nabla(k\nabla T)+S \quad (3)$$

where ρ is the density of the PCM, $\overline{v}$ is the fluid velocity, k is the thermal conductivity, H is the enthalpy, and S is the source term.

The sensible enthalpy can be expressed as

$$h=h_{\mathrm{ref}}+\int_{T_{\mathrm{ref}}}^{T} cp\Delta T, \quad (4)$$

and H can be defined as

$$H=h+\Delta H, \quad (5)$$

where h_{ref} is the reference enthalpy at the reference temperature T_{ref}, cp is the specific heat, ΔH is the latent heat content that may change between zero (solid) and 1 (liquid), L is the latent heat of the PCM, and γ is the liquid fraction that occurs during the phase change between the solid and liquid state when the temperature is $T_l > T > T_s$. Thus, γ may be written as

$$\gamma=\Delta H/L, \quad (6)$$

$$\gamma=\begin{cases}0 & \text{if} \quad T<T_s\\ 1 & \text{if} \quad T>T_l\\ (T-T_s)/(T_l-T_s) & \text{if} \quad T_l>T>T_s\end{cases} \quad (7)$$

The source term S_i in momentum equation, is defined as

$$S = C\,(1-\gamma)^2 \frac{\overline{v}}{\gamma^3 + \epsilon} \tag{8}$$

It is the Darcy's law damping terms (as source term) that are added to the momentum equation due to phase change effect on convection. Where $\epsilon = 0.001$ is a small computational constant used to avoid division by zero, the mushy zone constant C describes the kinetic process in the mushy zone ordinary between 10^4 and 10^7.

2.3. Fluent solver

The Fluent software has two main solvers: the pressure-based solver and the density-based coupled solver (DBCS). Only the first method can be used to simulate the melting and solidification

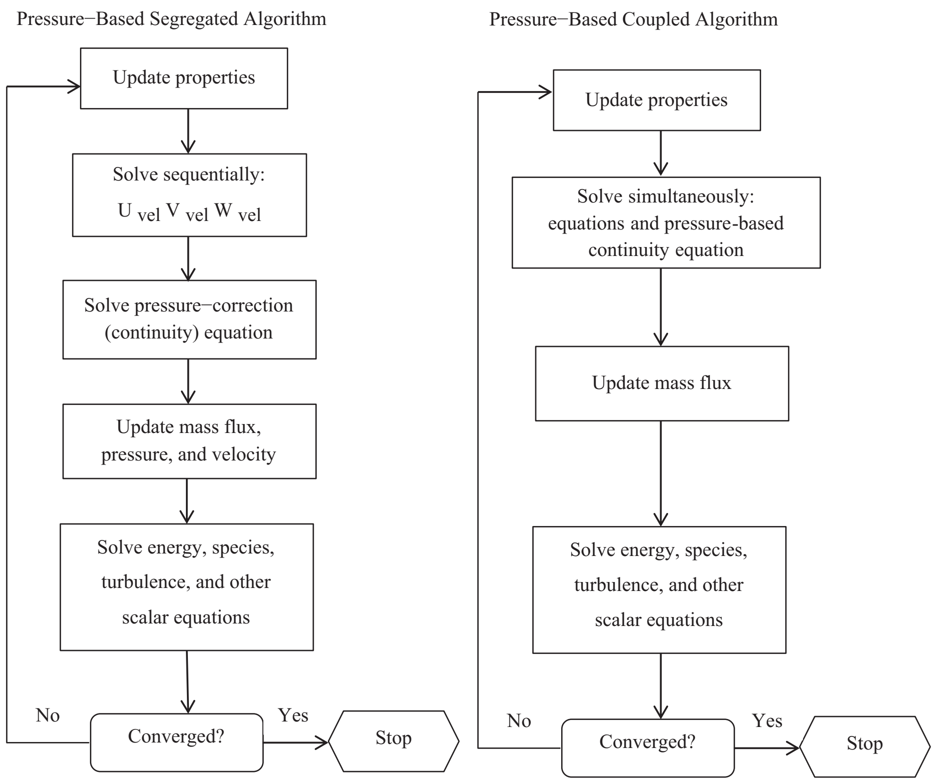


Fig. 2. Overview of the pressure-based solution methods [25].

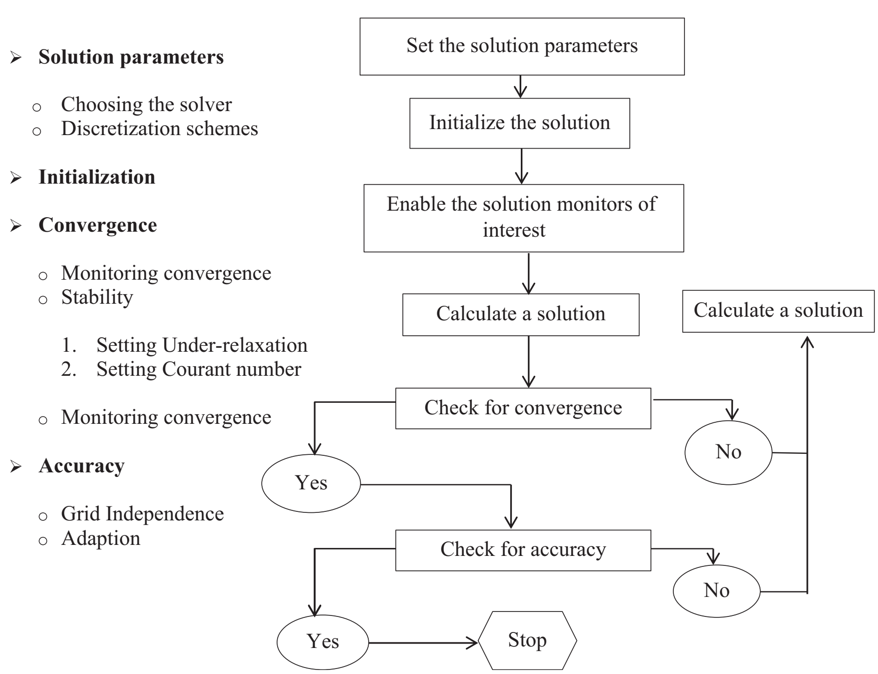


Fig. 3. Solution procedure overview for Fluent [30].

problems. The pressure-based solver employs an algorithm that belongs to a general class of methods called the projection method [29] wherein the constraint of the mass conservation (continuity) of the velocity field is achieved by solving a pressure (or pressure correction) equation. The pressure equation is derived from the continuity and the momentum equations in such a way that the velocity field, corrected by the pressure, satisfies the continuity. The governing equations are nonlinear and coupled to one another; thus, the solution process involves iterations where the entire set of governing equations is solved repeatedly until the solution converges. Available in Fluent are two pressure-based solver algorithms, namely, a segregated algorithm and a coupled algorithm Fig. 2.

Different discretization (interpolation methods) schemes are available for the convection terms in Fluent, including the first-order upwind scheme, power law scheme, second-order upwind scheme, central-differencing scheme, and the quadratic upwind interpolation scheme. The first-order upwind, power law, and second-order upwind schemes are mostly used with solidification and melting problems. The last two methods are more accurate than the first methods. In addition, the interpolation method of the face pressure for the momentum equations are the semi-implicit pressure-linked equation (SIMPLE), the SIMPLE-consistent (SIMPLEC), the pressure-implicit with splitting of operators (PISO), and the fractional step method (FSM). Fig. 3 shows the solution procedure overview. More details about the solution, initialization, and discretization methods can be found in Ref. [25].

The physical properties of materials, such as density, thermal conductivity, heat capacity, and viscosity, may be temperature-dependent and/or composition-dependent. The temperature dependence is based on a polynomial, piecewise-linear, or piecewise-polynomial function. Individual component properties are either defined by the user or computed via kinetic theory. Nevertheless, these physical properties can be defined as a constant value, a temperature-dependent function, or a user-defined function (UDF) that can be written in a specific programming language to define the temperature-dependence of the thermophysical properties.

Some researchers deduced that the thermophysical properties of PCMs, such as density and viscosity, are dependent on temperature changes and are determined by specific correlations.

$$\rho = \rho_1/(\beta(T-T_1)+1) \tag{9}$$

$$\mu = \exp(A+B/T) \tag{10}$$

Where ρ_1 is the density of PCM at the melting temperature T_l, β is the thermal expansion coefficient, and A, B are constant coefficients. The relationship between PCM and air is described by a specific model called the volume of fluid (VOF). This model defines the PCM–air system with a moving internal interface, but without inter-penetration of the two-phase fluid. Three conditions reflect the fluid's volume fraction in the computational cells, denoted as α_n: if $\alpha_n=0$, then the cell is empty of the nth fluid; if $\alpha_n=1$, then the cell is full of the nth fluid; and if $0<\alpha_n<1$, then the cell contains the interface between the nth fluid and one or more other fluids.

Shmueli et al. [31] numerically investigated the melting of PCM in a vertical cylinder tube with a diameter of 3 and 4 cm, exposed to air above, and insulated at the bottom. The wall temperature was between 10 and 30 °C above the melting

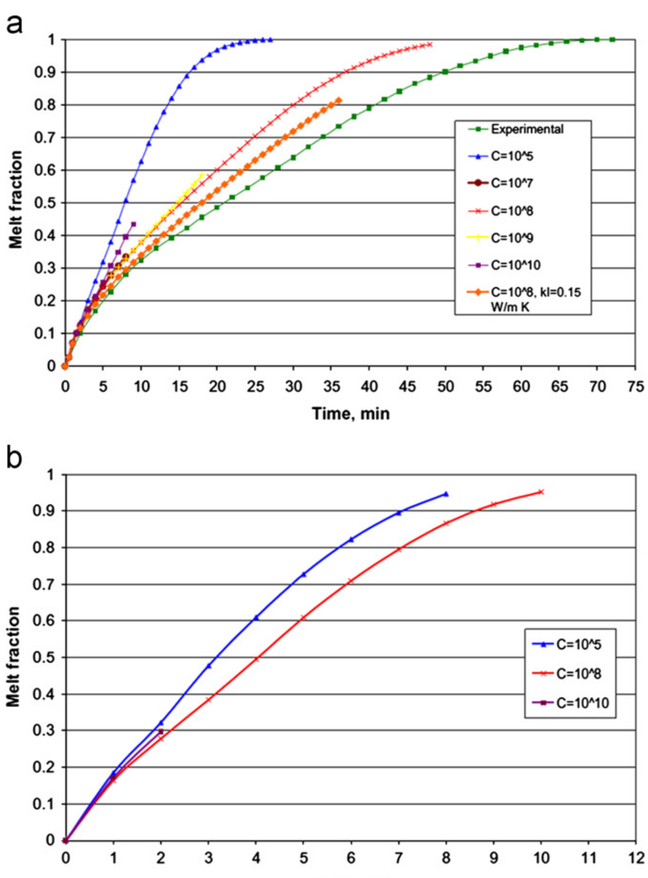


Fig. 4. Melt fraction vs. time for various values of the mushy zone constant with different models [31].

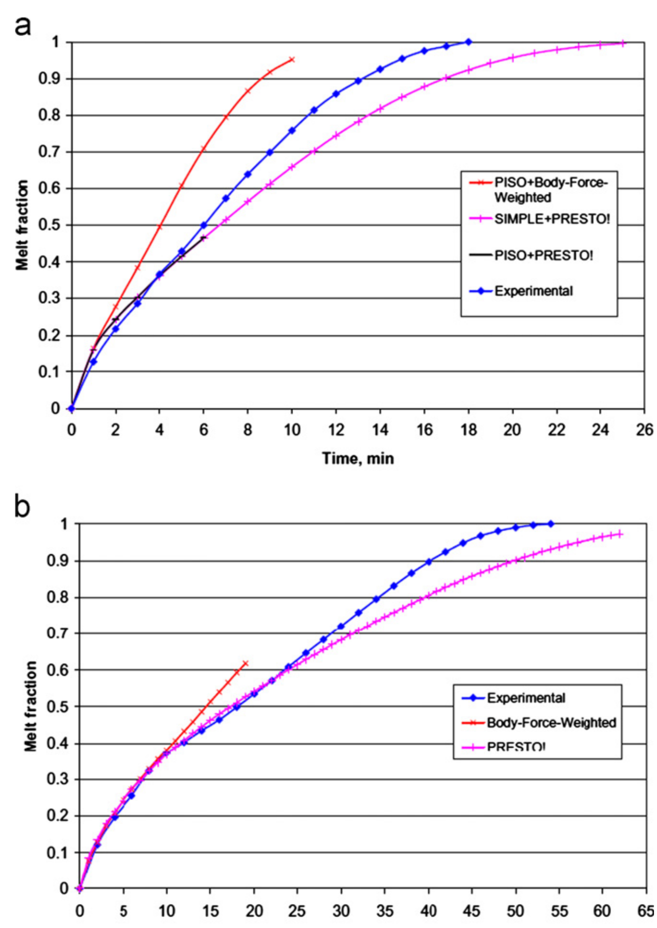


Fig. 5. Comparison between pressure discretization schemes and experimental results with different models [31].

temperature of the PCM. They studied the effect of various numerical solution parameters such as the pressure velocity scheme (PISO and SIMPLE) and the pressure discretization regime (e.g., PRESTO and the weighted force method). They analyzed the influence of the mushy zone constant to the melting process, as shown in Fig. 4 and Fig. 5. They also reported no difference in the pressure velocity scheme (PISO and SIMPLE) as well as a considerable difference in the result for pressure discretization.

3. Numerical simulation of PCM in thermal storage geometries

3.1. Spherical capsule geometry

LHTES in a spherical container represents an important case for thermal storage to be used in different engineering applications such as in packed-bed storage. Moreover, most commercial companies produce the spherical capsule for this application.

Assis et al. [32] presented a numerical and an experimental investigation of the melting process of RT27 with a PCM in a spherical geometry filled with 98.5% solid PCM as an initial condition of the simulation. One percent was left to account for the increase of the PCM volume during the phase change transition. The variable density was defined during the liquid state with linear variation in the "mushy" state, and the VOF was used for the PCM–air system. The numerical model was based on the axial symmetry of the physical model using Fluent 6.0. Different design and operation parameters were studied, and the results indicated that the melting process of the PCM is affected by its thermal and geometrical parameters, including the Stefan number and the shell diameter. Assis et al. [33] numerically and experimentally studied the solidification process of RT27 as a PCM in a spherical shell filled with 98.5% liquid PCM. Different shell diameters were examined, and a transient numerical model was developed using Fluent 6.2; the numerical model was the same one used in the melting process of PCM [32].

Hosseinizadeh et al. [34] numerically studied the effect of various volume fractions of nanopractical copper on an unconstrained melting rate in a spherical container. Different volumes of nanopractical copper (0, 0.02, 0.04) per volume were used, and 85% of the PCM was filled. They used Fluent to develop an axisymmetric numerical model and added the Darcy law to the momentum equation to account for the effect of phase change on convection. The VOF used for the PCM–air system and the power law scheme and the PISO method used for the pressure–velocity coupling were adopted to solve the momentum and energy equations, respectively. The PRESTO scheme was used for the pressure correction equation. Three different Stefan numbers were analyzed; the validation of the model was based on the experimental work by Assis et al. [32]. The results indicated that the nanopractical copper caused an increase in the thermal conductivity of the nano-enhanced PCMs compared with the conventional PCM. Unfortunately, the latent heat of fusions decreased.

Tan et al. [35] reported an experimental and numerical work on the constrained melting of PCM inside a transparent spherical glass capsule. The Darcy law was added to the momentum equation to account for the effect of phase change on convection. They used Fluent 6.2.16 for the numerical simulation and the SIMPLE method for solving the governing equations. The power law differencing scheme was used to solve the momentum and energy equations, whereas the PRESTO scheme was adopted for the pressure correction equation. They reported that waviness and excessive melting of the bottom of the PCM was underestimated by the experimental observation. This discrepancy was linked to the use of a support structure to hold the sphere that could have inhibited heat from reaching the bottom of the sphere.

Xia et al. [36] developed an effective packed-bed thermal energy storage that contains a spherical PCM capsule. They studied the effect of the arrangement of the PCM spheres and the encapsulation of the PCM on the heat transfer performance of the LTES bed. They developed a 2D numerical model via Fluent 6.2 using the standard k–ξ model for turbulent flow; a SIMPLE algorithm was adopted for pressure and velocity coupling. They reported that random packing was more favorable than special packing for heat storage and retrieval; both the material and the thickness of the encapsulation had apparent effects on the heat transfer performance of the LTES bed.

3.2. Square and rectangular geometry

Arasu and Mujumdar [37] presented a numerical investigation on the melting of paraffin wax dispersed with aluminum (Al_2O_3) as a nano-PCM in a square enclosure heated from the bottom side and from a vertical side with different volume percentages (2% and 5%). They developed a numerical model using Fluent 6.3.26. The computational domain was resolved with a fine mesh near the hot and cold wall to resolve the boundary layer; an increasingly coarser mesh was used in the rest of the domain to reduce computational time. They used a UDF to define the temperature-dependence of the thermophysical properties of PCM, wherein the first-order upwind difference scheme was used to solve the momentum and energy equations, and the PRESTO scheme was adopted for the pressure correction equation. They reported that the effective thermal conductivity of a paraffin wax latent heat storage medium could be increased significantly by smaller volumetric concentrations of alumina particles in the paraffin wax.

Pinelli and Piva [38] developed a 2D numerical model using Fluent to study the effects of natural convection on the PCM process in terms of temperature distributions, interface displacement, and energy storage, and to enhance the agreement between the experimental work with the numerical one when the conduction dominated is considered only for the heat transfer of the PCM. The mushy zone constant for the model was approximately $1.6*10^3$, and the cylinder cavity was filled with n-octadecane as PCM in the solid state and heated from above with an electrical heater. The overall heat transfer coefficient U considered conduction through the polystyrene layer as well as the convection and radiation heat exchanged with the environment. The model was validated with an analytical solution wherein the conduction-dominated freezing and numerical methods were considered in the convection–conduction. They reported that the agreement between numerical and experimental results significantly improved when the presence of circulation in the liquid phase, instead of in the conduction-dominated process only, was considered.

Researchers reported that the heat transfer in PCM could be enhanced significantly by adding nanopractical copper to the PCM (nanofluid). Such addition improves the PCM's thermal conductivity. Wu et al. [39] numerically investigated the melting processes of Cu/paraffin nanofluid PCMs. They developed a 2D numerical model using Fluent 6.2. The enclosed cavity was filled with 2.5-cm high PCM and 1 cm air; the top of the cavity was enclosed and taken by air. The VOF was adopted to describe the relationship between the PCM and air with a moving interface, but without inter-penetration of the two media. The QUICK differencing scheme was used to solve the momentum and energy equations, whereas the PRESTO scheme was adopted for the pressure correction equation. They reported a 13.1% decrease in the paraffin's melting time.

Li et al. [40] numerically studied the melting process of a PCM in concentric horizontal annuli of a square external shell. A 2D numerical model was adopted using Fluent 6.0. They reported that the top part of the PCM melts faster than the bottom part as a result of the convection-dominated mode, which accelerates the melting of the top part of the annulus.

Khodadadi and Hosseinizadeh [41] reported that the dispersion of nanoparticles in PCMs enhanced the material's thermal conductivity in contrast to the base material. They used a 2D numerical model within the commercial code of Fluent 6.2.1. The SIMPLE algorithm and the QUICK differencing scheme were used to solve the momentum and energy equations, whereas the PRESTO scheme was adopted for the pressure correction equation. The Darcy Law damping terms were added to the momentum equation. The results indicated an increase in the thermal conductivity of the nano-enhanced PCMs in contrast to the conventional PCM. Unfortunately, the latent heat of fusion decreased.

3.3. Cylindrical capsule geometry

Cylindrical geometries are considered most promising for devices for commercial heat exchangers, such as the double pipe heat exchanger and shell and the tube heat exchanger, because of their high-efficiency in a minimum volume. Most researchers use this geometry for LHTES, filling the PCM in the tube side or in the annulus (shell). Commercial products of PCMs are delivered in these geometries.

Darzi et al. [42] used Fluent 6.2 to simulate the melting process of the n-octadecane as a PCM in the concentric and eccentric double pipe heat exchanger. They studied the effect of the internal tube position on the melting rate. They developed a 2D numerical model (R, θ) and adapted low power to solve the momentum and energy equations. The SIMPLE method was used for pressure–velocity coupling, and the PRESTO scheme was used for the pressure correction equation. The results indicated that the melting rate was the same in the early stage of melting, and then decreased in the concentric model.

Gou and Zhang [43] reported that the solidification process of KNO_3–$NaNO_3$ as PCM in solar power generation using the direct steam technology is controlled by pure conduction. They neglected the influences of natural convection when comparing it with heat conduction. They developed a 2D numerical model via Fluent 6.2 and studied the storage with and without foil based on the same tube diameters and PCM. The results indicated how the heat transfer and discharge time were affected by the changes in the geometry of the aluminum foil and in the tube radius. They reported that the discharge process significantly accelerated with the addition of the aluminum foil.

Colella et al. [2] designed a medium-scale LHTES unit for district heating systems. The shell-and-tube LHTES that included RT100 as a PCM in the shell side was used to transfer heat from the district to the heating networks of the building; the heat transfer fluid was water. The thermal storage was charged during the night using CHP plants and then discharged during the day at the peak of the thermal request. A 2D numerical model (R, X) was developed using the Fluent simulation software to study the thermal behavior of the PCM and the HTF. Grid meshing of the computational model was refined systematically. The SIMPLE algorithm was adopted to solve the pressure–velocity coupling. The second-order upwind scheme was used for the convective fluxes. A naturally expanded graphite matrix with 15% volume was added to the paraffin to enhance the thermal conductivity of the composite (paraffin–graphite) to achieve the heat fluxes required for the medium scale application. Different operation strategies and parameters were studied, including the time-wise variation of the liquid fraction, PCM temperature, and the HTF outlet temperature. Based on their analysis, the best options for energy storage density were characterized by latent storage units installed on the heating network of the building rather than on the primary district heating network.

Buyruk et al. [44] studied the solidification process of water around different staggered and inline cylinders placed in a rectangular ice storage tank. They developed a 2D numerical model using Fluent to depict the temperature distributions and ice formation in the tank. They adopted Darcy's law and the Kozeny–Carman equation to model the flow and permeability of the mushy zone, respectively. Based on a fixed ice storage tank volume, the solidified area of four inline cylinders was larger than that for six inline cylinders.

4. Numerical simulation of the PCM applications

4.1. Numerical simulation of PCM for electronic devices applications

Shatikan et al. [45] numerically presented the melting process of a PCM with internal fins exposed to air from the top and heated from the horizontal base. They investigated different fin dimensions with a constant ratio between the fin and the PCM thickness. They used Fluent 6.0 to develop 2D and 3D numerical models and adopted the VOF model to describe the relationship between the air and the PCM; the SIMPLE algorithm was used for the pressure–velocity coupling. The 2D model was considered because the 3D model was time consuming. They reported that the results for the 2D and 3D models were equal in some dimensions, and the transient phase change process of the PCM depended on the operation and design parameters of the system. Such parameters were related to the temperature difference between the base and the mean melting temperature, as well as to the thickness and height of the fins. Shatikian et al. [10] analyzed the same model with constant heat flux applied from the horizontal base.

Wang and Yang [11] numerically studied the cooling technology of portable handheld electronic devices using PCM. They developed half computational grids with the 3D numerical model using Fluent 12 to investigate the effect of a different amount of fins and various power's heating level. They adopted the VOF model to describe the relationship between the air and the PCM. In the VOF model, the Geo-Reconstruct, which is the volume fraction discretization scheme, was used to calculate the transient moving boundary. If the transient temperature of the calculation cell in the PCM domain was equal to or higher than the melting temperature, the continuity and momentum equations were calculated in the system; the SIMPLE algorithm was used for the pressure–velocity coupling. They studied the orientation of PCM with the heat sink; the model was validated using the method by Fok et al. [46]. The numerical results indicated that the orientation had insufficient influence on the transient thermal performance of the hybrid cooling system, and that the transient surface temperature caused a discrepancy of around 8.3%–10.7%. They reported that PCM in aluminum heat sink with six fins could provide stable temperature control and good cooling ability.

Yang and Wang [12] numerically investigated the cooling technique using a hybrid PCM-based heat sink within a closed system to absorb constant and uniform volumetric heat generated from portable handheld electronic devices. They tested different computation grids and time steps to validate the model with the experimental work; various power levels (2–4 W), different orientations (vertical, horizontal, slanted), as well as charging and discharging times were conducted in the simulation model. The melting rate increased when a higher power level was transferred to the system. They reported that the maximum

temperature of the hybrid system using PCM could be well controlled under 320 K if the melting ratio was under 0.9 or if the melting time was shorter than 6801.2 s.

Ye et al. [47] figured out the correlation between influential variables, such as the liquid fraction and thermal storage time, the transient heat flux and melting period, and the solid fraction and the solidification time by numerically studying the heat transfer and fluid flow in a plate fin filled with PCM for rapid heat absorbed/released techniques. They developed a 2D numerical model through Fluent. The cavity was filled with 85% PCM and 15% air to consider thermal expansion during the solid–liquid phase change; finely structured meshing grids were installed near the heating and cooling plate wall to resolve the boundary layers. The VOF model was adopted to describe the relationship between the air and the PCM. The UDF was written in C language to account for the temperature dependence of the thermophysical properties. The SIMPLE algorithm was considered for the pressure–velocity coupling, and different time steps were used for the energy storage and energy release. Exploring via a 3D numerical model, they reported no difference in the results between the 2D and 3D models. The correlations they obtained will be useful for future component design and system optimization.

Ye et al. [48] performed further studies on the effect of PCM cavity volume fraction on the heat transfer behavior and fluid flow in LHTES. Different parameters of LHTES performance, such as the volume expansion ratio, the time of complete thermal storage, heat flux, liquid fraction, and velocity and temperature fields, were investigated. They used the same model in Ref. [47], except that the time step was chosen in relation to the grid size via the Courant–Friedriches–Lewy number. They reported that the volume expansion ratio decreased as cavity volume fraction x increased. By contrast, the time for complete energy storage increased.

Kandasamy et al. [49] numerically and experimentally investigated the use of a PCM-based heat sink for quad flat package (QAP) electronic devices. They developed one quarter of the physical model as well as a 3D numerical model using the commercial Fluent 6.2. The VOF was used to describe the relationship between the air and the PCM. The PISO scheme was used for the pressure–velocity coupling. The cooling performance of the PCM-based heat sinks improved, compared with the case without PCM. The full melting of the PCM and the melting rate also increased as the input power increased.

Sabbah et al. [50] presented the thermal and hydraulic behavior of a micro-channel heat exchanger with MCPCM water slurry for heat dissipation of a high-power electronic device. They developed a 3D numerical model using Fluent 6.2, and the SIMPLE algorithm was used for velocity–pressure coupling. The heat transfer in both the cooling fluid and the metal heat sink on the overall performance of the system was considered. The results showed a significant increase in the heat transfer coefficient that depended on the channel inlet and outlet and on the selected MCPCM melting temperatures. Lower and more uniform temperatures throughout the electronic device could be achieved using less pumping power compared with the case using only water as the cooling fluid.

Hosseinizadeh et al. [51] numerically and experimentally presented the thermal management of electronic products using PCM. They compared the effect of the PCM cooling technology in contrast to the normal ones. Different design parameters were studied to determine their effects on the temperature of the heat sink and on the melting of PCM inside the heat sink. 85% of the heat sink height was filled with PCM, and 15% of the height was modeled in the air region for the solid-to-liquid conversion in the PCM expansion. A 2D numerical model was adopted via Fluent. Density was considered constant in the solid state, whereas liquid density was a function of the temperature and the thermal expansion coefficient. The VOF was adopted to describe the PCM–air system. The PISO algorithm was used for the pressure–velocity coupling. They set the time step at 0.0001 s at the early stage of simulation and changed it to 0.001 s after 3 min of simulation. The increased fin thickness showed only a slight improvement in thermal performance, whereas an increase in the number of fins and fin height resulted in an appreciable increase in the overall thermal performance.

4.2. Numerical simulation of PCM for HVAC equipment

Tay et al. [52] modeled different tube configurations in a shell and tube heat exchanger with PCM in the shell side. They developed a 3D CFD model using ANSYS code to analyze the transient heat transfer during the phase change process. Three grid resolutions were evaluated for the tube, HTF, and PCM. ANSYS CFX 12.1 was used to complicate the physical properties of the mixture. Three domains were created using CFX.PRE version 12.1, namely, liquid for HTF, liquid for PCM, and solid for the tube. An experimental apparatus was developed to compare the predicted simulation results of both freezing and melting processes. They found that the results of the CFD melting model were generally longer than the experimental results. The thermal behavior of the freezing and melting processes of PCM was different from those in the experimental results when the natural convection was ignored.

Antony and Velraj [53] studied the heat transfer and fluid flow through a tube in a regenerative PCM heat exchanger (shell and tube) module incorporated into a ventilation system. The PCM was encapsulated in the shell side of the module for a free cooling system. Fluent software was used to analyze the heat transfer and flow through the model, which consisted of an air flow passenger and two air spacers on top and at the bottom. PISO algorithm was adopted for the pressure–velocity coupling. The second-order upwind scheme was used for the approximation of the convective terms. The k–ξ model was used for the turbulence modeling of the heat transfer fluid. This module was validated experimentally. The results from the experiment and the calculated results were compared.

Xia and Zhang [54] prepared an acetamide/expanded graphite composite (AC/EG) with 10% (mass fraction) as PCM to be used in active solar applications, such as solar-driven solid/liquid desiccant dehumidification systems and solar-driven adsorption/absorption refrigeration systems that require a higher heat source temperature of over 60 °C. They measured the thermal properties, including melting/freezing points, thermal conductivities, and the heat of fusion, using the transient hot-wire method and a differential scanning calorimeter. Two-thirds of the test model was filled with solid PCM for the thermal expansion during the solid–liquid phase change. They developed a 2D numerical model using Fluent 6.2 to study the release and absorption of heat in LHTES. The numerical model was validated experimentally. The thermal conductivity of the composite AC/EG (2.61) was six times that of pure metal; 0.043 for solid at 60 °C and 0.2 for liquid at 90 °C. The phase change temperature shifted and the latent heat decreased compared with that of pure AC. The heat storage and retrieval durations of the LTES unit with the AC/EG composite showed 45% and 78% reductions, respectively, compared with those for pure AC.

New internal fins inside spherical and cylindrical PCM encapsulation in the HVAC system for buildings were numerically investigated by Siva et al. [55]. They developed a numerical model using Fluent 6.3 to study the charging and discharging process of PCMs for the two configurations. Incorporating fins for

different configurations reduced the total solidification time by 65%–72%.

4.3. Numerical simulation of PCM for building applications

LHTES is used extensively in building structures to remove thermal load and to improve the thermal comfort of occupants. PCM can be found in different items of the building structure, such as the walls, roof, floor, ceiling, window shutters, plasterboard, and tiles. Most researchers mentioned in the present study used CFD to simulate the process, reporting a good agreement between the simulation and the experimental results.

Silva et al. [56] incorporated a PCM into a typical clay brick masonry enclosure wall in Portugal as a passive technology to enhance the building's energy efficiency. They experimentally and numerically evaluated how the PCM reduced internal temperature fluctuations and increased the time delay between internal and external conditions. They generated the mesh grid in CFD and developed a 2D numerical model in ANSYS Fluent 12. The SIMPLE algorithm was used to solve the governing equations. The second-order upwind scheme was used to solve the pressure, momentum, and energy equations. They reported that incorporating the PCM into the wall contributed to the attenuation of the indoor space temperature swing, which reduced from 10 to 5 °C, and to the thermal amplitude. The time delay also increased by approximately 3 h.

Joulin et al. [6] analyzed the energy conservation of a building with PCM conditioned in a parallel epipedic polyfin envelope to be used in passive solar walls. They developed a 1D Fortran numerical model and a 2D model using commercial Fluent to study the thermal behavior of the PCM to validate the experimental work. The self-developed numerical model was based on the enthalpy formulation and on the fully implicit finite difference solution method used for discretization. The equations were solved using TDMA. The liquid fraction was updated in each iteration until convergence was achieved. For the commercial Fluent, the SIMPLE method was used to solve the governing equations. The power law differencing scheme was used to solve the momentum and energy equations, whereas the PRESTO scheme was adopted for the pressure correction equation. They reported that the 1D and 2D numerical simulations did not satisfy because the results were very far from the experimental ones: the codes did not represent the supercooling phenomenon. Numerical modeling showed that the supercooling phenomenon must be taken into account correctly to predict the PCM thermal behavior.

Susman et al. [57] constructed four 150 mm^2 prototype PCM sails from paraffin/low-density-polyethylene composites installed below the ceiling of an occupied office space in London in the summer. During daytime, the modules were hung on an internal rig 2.5 m above the ground; after 8 p.m., the modules were transferred to the outside rig to discharge the energy, and were moved to the inside rig at 7 a.m. They developed a semi-empirical model of the modules in Fluent using an enthalpy–porosity formulation to model phase change. The modules were validated well using the temperature measurements, including a notable divergence when the maximum liquid fraction was reached.

4.4. Numerical simulation for other applications

Bo et al. [58] introduced a metal PCM energy storage in a high-temperature heat pipe steam boiler used for direct steam generation in a solar thermal power generation system. The Al–Si eutectic alloy contained 12.07% Si used as a PCM at a melting temperature of 577 °C The temperature distributions of the heat reservoir tank and the heat storage medium under high solar heat flux were analyzed using a 2D numerical model via Fluent. The newly developed heat storage boiler could withstand a focused solar energy flux of 400 kW/m^2 and was compatible with the heat storage medium.

Tan et al. [16] used water as a PCM to recover and store cold energy from a cryogenic gas in a cryogenic cold energy system. They developed a 2D numerical model using Fluent to analyze the effect of the thermal boundary and thermal resistance on the freezing process in an LHTES system. Their numerical model was based on half the domain because the geometrical model was considered symmetric. The standard k–ξ model was adopted to calculate the internal forced convection of the gaseous coolant. The CFD model was validated experimentally and showed good agreement with the experimental results. They reported that the dimensionless numbers, such as the Biot number and the Stefan number of the PCM, and the Stanton number of the coolant flowing in the tube had a noticeable influence on the PCM freezing characteristics. A larger Biot number was beneficial to the heat transfer between the PCM and the coolant, promoting a higher freezing rate. A higher Stefan number appeared to result in larger freezing rates in a fixed axial position. Moreover, the frozen layer slope along the tube was steeper at larger Stanton numbers.

Xiaohong et al. [59] numerically studied a PCM at high melting temperatures (1120 K) in a heat pipe receiver in an advanced solar dynamic power generation system. A 2D numerical model was adopted via Fluent 6.2 to simulate the heat transfer of the PCM canister of the heat pipe receiver. UDF was used in the simulation. The numerical results were compared with NASA's numerical results. The temperature of the heat pipe wall and the outer wall of the PCM canister in the numerical model and in the NASA simulation differed only slightly. These results can be used to guide the design and optimization of PCM canisters for heat pipe receivers.

Koizumi and Jin [60] proposed a new compact slab container with an arc outer configuration to promote direct contact melting. They studied two configurations of the close contact melting process, namely, flat slab container and curved slab container. The 2D numerical model was performed via Fluent 6.3. The VOF model was adopted to describe the PCM–air system. A first-order accurate upwind difference scheme was adopted for the convection terms because the convection velocity in the liquid PCM was extremely small (within several mm/s). The simulated results quantitatively elucidated the experimental melting process from beginning to end.

MacPhee and Dincer [61] numerically investigated and thermodynamically analyzed the melting and solidification process of a de-ionized water as PCM in a spherical capsule geometry. They developed a 3D model using Fluent 6.0 and studied the effect of the HTF inlet temperature and the flow rate. The numerical model was validated and was found to be in good agreement with the experimental data. The variations of the incoming HTF temperature had a much larger effect on the charging times and on the energy and exergy efficiencies compared with the changing of the HTF flow rate.

Reddy [62] presented a solar-integrated collector storage water heating system with PCM to optimize the solar gain and heat loss characteristics through a 2D numerical model using commercial Fluent and UDF to express the variable heat flux condition on the absorber plate. Different numbers of fins were attached to the PCM water solar system to enhance the heat transfer. The latent heat storage with nine fins was optimal at maximum water temperature and had minimum heat loss to the surroundings.

Rao et al. [63] discussed the use of PCM with an aging commercial $LiFePO_4$ power battery to study the thermal behavior of the PCM and the cell for thermal energy management. They developed a 3D computation model for a single cell and a battery package using the commercial computational Fluent. They

reported that the design for battery thermal management should include a proper selection of the thermal conductivities for the PCM and the cell because the thermal conductivity increased, whereas the latent heat of fusion decreased.

Darkwa and Su [64] studied the effect of particle distribution on the thermal performance of micro-encapsulated PCMs in different configurations of a composite high conductivity laminated MCPCM board. They developed a 3D numerical model using Fluent 6.3. The SIMPLE algorithm was used for the pressure–velocity coupling, and the second-order upwind scheme was adopted for both momentum and energy equations. The PRESTO pressure discretization scheme was used for the pressure correction equation. The thermal response times for the rectangular and triangular geometries were approximately half of that for the pyramidal geometry during the cooling and heating processes of the board.

MacPhee et al. [65] numerically studied the effect of different capsule geometries, HTF inlet temperatures, and HTF flow rates on energy and exergy efficiencies for the solidification process in encapsulated ice thermal energy storage (EITES). They used Fluent 6.3 to simulate different geometries (slab, cylindrical, spherical), three HFT flow rates, and three HTF inlet temperatures to achieve the highest efficient charge method for the thermal storage. They recommended the exergy efficiency methods to study system performance, stating that these methods provide better insight into system losses. They also advised EITES designers to increase both the flow rate and inlet HTF temperature to achieve full system charging in an acceptable amount of time.

5. Conclusion

The sustainable thermal energy storages for different engineering applications, such as building structures and HVAC equipment, are indispensable to reducing greenhouse-gas emission. LHTES is an important component of thermal solar engineering systems, playing a key role in improving the energy efficiency of these systems. Thermal energy storage systems, especially LHTES, have gained widespread attention in relation to global environmental problems and energy-efficiency improvement. The following conclusions can be summarized for CFD applications in latent heat thermal storage.

1. The numerical solution for the PCM phenomena is more accurate than the analytical solution and can be used in different engineering conditions.
2. The CFD software is used successively to simulate the application of PCM in different engineering applications, such as electronic cooling technology, building thermal storages, and HVAC.
3. Different CFD software are used in PCM engineering, including ANSYS Fluent, Comsol Multiphysics, and Star-CCM+. The most commonly used software is ANSYS Fluent.
4. The numerical results of the 2D numerical model are generally the same as those of the 3D numerical model. Researchers reported that the time required for simulation was reduced.
5. The application of CFD in designing PCM thermal storages is a feasible method because of the highly accurate results of the experimental work. CFD also delivers optimization tools to help users achieve maximum efficiency while saving time and money.

References

[1] Al-Abidi AA, Bin Mat S, Sopian K, Sulaiman MY, Lim CH, Th A. Review of thermal energy storage for air conditioning systems. Renewable and Sustainable Energy Reviews 2012;16:5802–19.
[2] Colella F, Sciacovelli A, Verda V. Numerical analysis of a medium scale latent energy storage unit for district heating systems. Energy 2012;45:397–406.
[3] Pasupathy A, Athanasius L, Velraj R, Seeniraj RV. Experimental investigation and numerical simulation analysis on the thermal performance of a building roof incorporating phase change material (PCM) for thermal management. Applied Thermal Engineering 2008;28:556–65.
[4] Meshgin P, Xi Y, Li Y. Utilization of phase change materials and rubber particles to improve thermal and mechanical properties of mortar. Construction and Building Materials 2012;28:713–21.
[5] Borreguero AM, Luz Sánchez M, Valverde JL, Carmona M, Rodríguez JF. Thermal testing and numerical simulation of gypsum wallboards incorporated with different PCMs content. Applied Energy 2011;88:930–7.
[6] Joulin A, Younsi Z, Zalewski L, Lassue S, Rousse DR, Cavrot J-P. Experimental and numerical investigation of a phase change material: thermal-energy storage and release. Applied Energy 2011;88:2454–62.
[7] Arnault A, Mathieu-Potvin F, Gosselin L. Internal surfaces including phase change materials for passive optimal shift of solar heat gain. International Journal of Thermal Sciences 2010;49:2148–56.
[8] Bony J, Citherlet S. Numerical model and experimental validation of heat storage with phase change materials. Energy and Buildings 2007;39:1065–72.
[9] F Cabeza L, Ibáñez M, Solé C, Roca J, Nogués M, Hiebler S, et al. Use of phase-change materials in solar domestic hot water tanks. ASHRAE Transactions 2006;112(1):495–508.
[10] Shatikian V, Ziskind G, Letan R. Numerical investigation of a PCM-based heat sink with internal fins: constant heat flux. International Journal of Heat and Mass Transfer 2008;51:1488–93.
[11] Wang Y-H, Yang Y-T. Three-dimensional transient cooling simulations of a portable electronic device using PCM (phase change materials) in multi-fin heat sink. Energy 2011;36:5214–24.
[12] Yang Y-T, Wang Y-H. Numerical simulation of three-dimensional transient cooling application on a portable electronic device using phase change material. International Journal of Thermal Sciences 2012;51:155–62.
[13] Çakmak G, Yıldız C. The drying kinetics of seeded grape in solar dryer with PCM-based solar integrated collector. Food and Bioproducts Processing 2011;89:103–8.
[14] Pandiyarajan V, Chinna Pandian M, Malan E, Velraj R, Seeniraj RV. Experimental investigation on heat recovery from diesel engine exhaust using finned shell and tube heat exchanger and thermal storage system. Applied Energy 2011;88:77–87.
[15] Oró E, Miró L, Farid MM, Cabeza LF. Improving thermal performance of freezers using phase change materials. International Journal of Refrigeration 2012;35:984–91.
[16] Tan H, Li C, Li Y. Simulation research on PCM freezing process to recover and store the cold energy of cryogenic gas. International Journal of Thermal Sciences 2011;50:2220–7.
[17] Azzouz K, Leducq D, Gobin D. Performance enhancement of a household refrigerator by addition of latent heat storage. International Journal of Refrigeration 2008;31:892–901.
[18] Azzouz K, Leducq D, Gobin D. Enhancing the performance of household refrigerators with latent heat storage: an experimental investigation. International Journal of Refrigeration 2009;32:1634–44.
[19] Mahmud A, K S, A. AM, Sohif M. Using a paraffin wax-aluminum compound as a thermal storage material in solar air heater. Journal of Engineering and Applied Sciences 2009;4:74–7.
[20] Sharma SD, Iwata T, Kitano H, Sagara K. Thermal performance of a solar cooker based on an evacuated tube solar collector with a PCM storage unit. Solar Energy 2005;78:416–26.
[21] Özisik MN. Finite difference methods in heat transfer. Boca Raton (Florida): CRC press, Inc; 1994.
[22] Dutil Y, Rousse DR, Salah NB, Lassue S, Zalewski L. A review on phase-change materials: mathematical modeling and simulations. Renewable and Sustainable Energy Reviews 2011;15:112–30.
[23] Joulin A, Younsi Z, Zalewski L, Rousse DR, Lassue S. A numerical study of the melting of phase change material heated from a vertical wall of a rectangular enclosure. International Journal of Computational Fluid Dynamics 2009;23:553–66.
[24] Verma P, Varun Singal S. Review of mathematical modeling on latent heat thermal energy storage systems using phase-change material. Renewable and Sustainable Energy Reviews 2008;12:999–1031.
[25] FLUENT 6.3 User's Guide, Fluent Inc. Lebanon; 2006.
[26] Voller VR, Prakash C. A fixed grid numerical modelling methodology for convection-diffusion mushy region phase-change problems. International Journal of Heat and Mass Transfer 1987;30:1709–19.
[27] Voller VR, Brent AD, Reid KJ. A computational modeling framework for the analysis of metallurgical solidication process and phenomena. Technical report. Conference for Solidication Processing. Ranmoor House, Sheffield; 1987.
[28] Voller VR. Modeling solidification processes. Technical report. Mathematical modeling of metals processing operations conference. Palm Desert (CA): American Metallurgical Society; 1987.
[29] Chorin AJ. Numerical solution of navier-stokes equations. Mathematics of Computation 1968;22:745–62.
[30] Solver Settings, Introductory FLUENT training v 6.3 Fluent User Services Center, ANSYS, Inc. Proprietary; December 2006.

[31] Shmueli H, Ziskind G, Letan R. Melting in a vertical cylindrical tube: numerical investigation and comparison with experiments. International Journal of Heat and Mass Transfer 2010;53:4082–91.
[32] Assis E, Katsman L, Ziskind G, Letan R. Numerical and experimental study of melting in a spherical shell. International Journal of Heat and Mass Transfer 2007;50:1790–804.
[33] Assis E, Ziskind G, Letan R. Numerical and experimental study of solidification in a spherical shell. Journal of Heat Transfer 2009;131:024502.
[34] Hosseinizadeh SF, Darzi AAR, Tan FL. Numerical investigations of unconstrained melting of nano-enhanced phase change material (NEPCM) inside a spherical container. International Journal of Thermal Sciences 2012;51:77–83.
[35] Tan FL, Hosseinizadeh SF, Khodadadi JM, Fan L. Experimental and computational study of constrained melting of phase change materials (PCM) inside a spherical capsule. International Journal of Heat and Mass Transfer 2009;52: 3464–72.
[36] Xia L, Zhang P, Wang RZ. Numerical heat transfer analysis of the packed bed latent heat storage system based on an effective packed bed model. Energy 2010;35:2022–32.
[37] Arasu AV, Mujumdar AS. Numerical study on melting of paraffin wax with Al_2O_3 in a square enclosure. International Communications in Heat and Mass Transfer 2012;39:8–16.
[38] Pinelli M, Piva S. Solid/liquid phase change in presence of natural convection: a thermal energy storage case study. Journal of Energy Resources Technology 2003;125:190.
[39] Wu S, Wang H, Xiao S, Zhu D. Numerical simulation on thermal energy storage behavior of Cu/paraffin nanofluids PCMs. Procedia Engineering 2012;31:240–4.
[40] Li W, Li X, Zhao J. Numerical study of melting in a square annulus. In: Proceedings of the mechanic automation and control engineering (MACE), 2010 International Conference; 2010. p. 891–4.
[41] Khodadadi JM, Hosseinizadeh SF. Nanoparticle-enhanced phase change materials (NEPCM) with great potential for improved thermal energy storage. International Communications in Heat and Mass Transfer 2007;34:534–43.
[42] Darzi AR, Farhadi M, Sedighi K. Numerical study of melting inside concentric and eccentric horizontal annulus. Applied Mathematical Modelling 2012;36: 4080–6.
[43] Guo C, Zhang W. Numerical simulation and parametric study on new type of high temperature latent heat thermal energy storage system. Energy Conversion and Management 2008;49:919–27.
[44] Buyruk E, Fertelli A, Sonmez N. Numerical investigation for solidificiation around various cylinder geometries. Journal of Scientific and Industrial Research 2009;68:122–9.
[45] Shatikian V, Ziskind G, Letan R. Numerical investigation of a PCM-based heat sink with internal fins. International Journal of Heat and Mass Transfer 2005;48:3689–706.
[46] Fok SC, Shen W, Tan FL. Cooling of portable hand-held electronic devices using phase change materials in finned heat sinks. International Journal of Thermal Sciences 2010;49:109–17.
[47] Ye W-B, Zhu D-S, Wang N. Numerical simulation on phase-change thermal storage/release in a plate-fin unit. Applied Thermal Engineering 2011;31: 3871–84.
[48] Ye W-B, Zhu D-S, Wang N. Fluid flow and heat transfer in a latent thermal energy unit with different phase change material (PCM) cavity volume fractions. Applied Thermal Engineering 2012;42:49–57.
[49] Kandasamy R, Wang X-Q, Mujumdar AS. Transient cooling of electronics using phase change material (PCM)-based heat sinks. Applied Thermal Engineering 2008;28:1047–57.
[50] Sabbah R, Farid MM, Al-Hallaj S. Micro-channel heat sink with slurry of water with micro-encapsulated phase change material: 3D-numerical study. Applied Thermal Engineering 2009;29:445–54.
[51] Hosseinizadeh SF, Tan FL, Moosania SM. Experimental and numerical studies on performance of PCM-based heat sink with different configurations of internal fins. Applied Thermal Engineering 2011;31:3827–38.
[52] Tay NHS, Bruno F, Belusko M. Experimental validation of a CFD model for tubes in a phase change thermal energy storage system. International Journal of Heat and Mass Transfer 2012;55:574–85.
[53] Antony Aroul Raj V, Velraj R. Heat transfer and pressure drop studies on a PCM-heat exchanger module for free cooling applications. International Journal of Thermal Sciences 2011;50:1573–82.
[54] Xia L, Zhang P. Thermal property measurement and heat transfer analysis of acetamide and acetamide/expanded graphite composite phase change material for solar heat storage. Solar Energy Materials and Solar Cells 2011;95:2246–54.
[55] Sivaa K, Lawrence MX, Kumaresh GR, Rajagopalan P, Santhanam H. Experimental and numerical investigation of phase change materials with finned encapsulation for energy-efficient buildings. Journal of Building Performance Simulation 2010;3:245–54.
[56] Silva T, Vicente R, Soares N, Ferreira V. Experimental testing and numerical modelling of masonry wall solution with PCM incorporation: a passive construction solution. Energy and Buildings 2012;49:235–45.
[57] Susman G, Dehouche Z, Cheechern T, Craig S. Tests of prototype PCM 'sails' for office cooling. Applied Thermal Engineering 2011;31:717–26.
[58] Bo ML, Yuan Z, Feng L, Sheng CG, Dong LS, Hong WC. Research of steam boiler using high temperature heat pipe based on metal phase change materials. In: Proceedings of the international conference on computer distributed control and intelligent environmental monitoring; 2011. p. 2208–12.
[59] Xiaohong G, Bin L, Yongxian G, Xiugan Y. Two-dimensional transient thermal analysis of PCM canister of a heat pipe receiver under microgravity. Applied Thermal Engineering 2011;31:735–41.
[60] Koizumi H, Jin Y. Performance enhancement of a latent heat thermal energy storage system using curved-slab containers. Applied Thermal Engineering 2012;37:145–53.
[61] MacPhee D, Dincer I. Thermodynamic analysis of freezing and melting processes in a bed of spherical PCM capsules. Journal of Solar Energy Engineering 2009;131:031017 [11 pages].
[62] Reddy KS. Thermal modeling of PCM-based solar integrated collector storage water heating system. Journal of Solar Energy Engineering 2007;129:458.
[63] Rao Z, Wang S, Zhang G. Simulation and experiment of thermal energy management with phase change material for ageing $LiFePO_4$ power battery. Energy Conversion and Management 2011;52:3408–14.
[64] Darkwa J, Su O. Thermal simulation of composite high conductivity laminated microencapsulated phase change material (MEPCM) board. Applied Energy 2012;95:246–52.
[65] MacPhee D, Dincer I, Beyene A. Numerical simulation and exergetic performance assessment of charging process in encapsulated ice thermal energy storage system. Energy 2012;41:491–8.
[66] Brent AD, Voller VR, Reid KJ. Enthalpy–porosity technique for melting convection-diffusion phase change:application to the melting of a pure metal. Numerical Heat Transfer 1988;13:297–318.
[67] Costa M, Buddhi D, Oliva A. Numerical simulation of a latent heat thermal energy storage system with enhanced heat conduction. Energy Conversion and Management 1998;39:319–30.
[68] Voller VR. Fast Implicit Finite-Difference Method for the Analysis of Phase Change Problems. Numerical Heat Transfer, Part B: Fundamentals 1990;17:155–69.
[69] Goodrich LE. Efficient numerical technique for one-dimensional thermal problems with phase change. International Journal of Heat and Mass Transfer 1978;21:615–21.
[70] Zukowski M. Mathematical modeling and numerical simulation of a short term thermal energy storage system using phase change material for heating applications. Energy Conversion and Management 2007;48:155–65.
[71] Zukowski M. Experimental study of short term thermal energy storage unit based on enclosed phase change material in polyethylene film bag. Energy Conversion and Management 2007;48:166–73.
[72] Trp A. An experimental and numerical investigation of heat transfer during technical grade paraffin melting and solidification in a shell-and-tube latent thermal energy storage unit. Solar Energy 2005;79:648–60.
[73] Lacroix M. Numerical simulation of a shell-and-tubelatent heat thermal energy storage unit. Solar Energy 1993;50:357–67.
[74] Esen M, Durmuş A, Durmuş A. Geometric design of solar-aided latent heat store depending on various parameters and phase change materials. Solar Energy 1998;62:19–28.
[75] Velraj R, Seeniraj RV, Hafner B, Faber C, Schwarzer K. Experimental analysis and numerical modelling of inward solidification on a finned vertical tube for a latent heat storage unit. Solar Energy 1997;60:281–90.
[75] Ismail KAR, Alves CLF, Modesto MS. Numerical and experimental study on the solidification of PCM around a vertical axially finned isothermal cylinder. Applied Thermal Engineering 2001;21:53–77.
[77] Tabassum TA. Numerical Study of a Double Pipe Latent Heat Thermal Energy Storage System. Montréal (Canada) McGill University; 2010.
[78] Kuehn TH, Goldstein RJ. An experimental and theoretical study of natural convection in the annulus between horizontal concentric cylinders. Jurnal of Fuid Mechanics 1976;74:695–719.
[79] Kuehn TH, Goldstein RJ. An experimental study of natural convection heat transfer in concentric horizontal cylindrical annuli. Journal of Heat Transfer 1978;100:635–40.
[80] Jian-you L. Numerical and experimental investigation for heat transfer in triplex concentric tube with phase change material for thermal energy storage. Solar Energy 2008;82:977–85.
[81] Ghoneim AA. Comparison of theoretical models of phase change and sensible heat storage for air and water-based solar heating systems. Solar Energy 1989;42(3):209–20.
[82] Adine HA, El Qarnia H. Numerical analysis of the thermal behavior of a shell-and-tube heat storage unit using phase change materials. Applied Mathematical Modelling 2009;33:2132–44.
[83] Gong Z-X, Mujumdar AS. Cyclic Heat Transfer in Novel Storage Unit of Multiple Phase Change Materials Applied Thermal Engineering 1996;16(10): 807–15.
[84] Fang M, Chen G. Effects of different multiple PCMs on the performance of a latent thermal energy storage system. Applied Thermal Engineering 2007;27:994–1000.
[85] Zhang Y, Faghri A. Semi-analytical solution of thermal energy storage system with conjugate laminar forced convection. International Journal of Heat and Mass Transfer 1996;39:717–24.
[86] Ismail KAR, Henríquez JR, da Silva TM. A parametric study on ice formation inside a spherical capsule. International Journal of Thermal Sciences 2003;42: 881–7.
[87] Ismail KAR. Moraes RIR. A numerical and experimental investigation of different containers and PCM options for cold storage modular units for domestic applications. International Journal of Heat and Mass Transfer 2009;52:4195–202.